AIAA 81-1297R

Effects of Sidewall Boundary Layers in Two-Dimensional Subsonic and Transonic Wind Tunnels

William G. Sewall*
NASA Langley Research Center, Hampton, Va.

A transonic similarity rule which accounts for the effects of attached sidewall boundary layers is presented and evaluated by comparison with the characteristics of airfoils tested in a two-dimensional transonic tunnel with different sidewall boundary-layer thicknesses. The rule appears valid provided the sidewall boundary layer both remains attached in the vicinity of the model and occupies a small enough fraction of the tunnel width to preserve sufficient two-dimensionality in the tunnel.

Introduction

THE interference of attached sidewall boundary layers in two-dimensional wind tunnels results in a modification to the continuity equation due to the reduction of the effective tunnel width by twice the sidewall boundary-layer displacement thickness. Methods for accounting for the effect have been proposed by Preston[1] and Winter and Smith,[2] where the presence of the sidewall boundary layer is considered as a change in the circulation about the airfoil. These methods have been concerned primarily with incompressible flow.

For subsonic and transonic compressible flow, this effect can be formulated into similarity rules which relate compressibility and the interaction effect of the sidewall boundary layer to the model-induced pressure field. This paper applies elements of the derivation of the similarity rule given by Barnwell[3] to the von Kármán transonic similarity rule, and presents results of a wind-tunnel experiment designed to evaluate the validity of the sidewall similarity rule at transonic speeds.

Analysis

Consider steady, isentropic, small-perturbation flow in a nominally two-dimensional airfoil wind tunnel. Let the Cartesian coordinates in the freestream, normal, and spanwise directions be x, y, and z and the respective velocity components be U, v, and w. The effective tunnel width is $b-2\delta^*$ where b and δ^* are the tunnel width and the sidewall displacement thickness, respectively. It is assumed that δ^* can vary slightly with respect to x and y and that the boundary conditions for the airfoil model and the upper and lower walls are independent of z. It is also assumed that the tunnel is narrow enough for the flow at each sidewall to be strongly influenced by the other sidewall boundary layer. To the lowest order, the spanwise velocity component in this tunnel varies linearly with the spanwise coordinate z as

$$w=\frac{-2Uz}{b}\frac{\partial\delta^*}{\partial x} \tag{1}$$

In wider tunnels the disturbance caused by the sidewall boundary layer decays nonlinearly with distance from the sidewall so that Eq. (1) is not valid.

The flow in the wind tunnel described above is governed by the small-perturbation form of the continuity equation, which can be written as

$$(1-M_\infty^2)\frac{\partial u}{\partial x}+\frac{\partial v}{\partial y}+\frac{\partial w}{\partial z}=(\gamma+1)M_\infty^2\frac{u}{U}\frac{\partial u}{\partial x} \tag{2}$$

where M_∞ is the freestream Mach number, $u=U-U_\infty$ is the velocity perturbation in the x direction, and γ is the ratio of specific heats of the gas.

The dynamics of the sidewall boundary layer are modeled with the von Kármán momentum integral, which can be written as

$$\frac{\partial\delta^*}{\partial x}=\frac{-\delta^*}{U}(2+H-M^2)\frac{\partial u}{\partial x}+\frac{\delta^*}{H}\frac{\partial H}{\partial x}+\frac{\tau_w}{\rho U^2} \tag{3}$$

where ρ is the density and δ^*, τ_w, and H are the sidewall displacement thickness, wall shear stress, and shape factor, respectively. For the present problem, Eq. (3) can be simplified because the sidewall boundary layer in most airfoil wind tunnels can be approximated as a flat-plate boundary layer with a large Reynolds number and an equivalent length of the order of $\delta^*/(\tau_w/\rho U^2)$. In general, the model chord c is much smaller than the boundary-layer equivalent length at the model station so that the inequality

$$\tau_w/\rho U^2 \ll \delta^*/c \tag{4}$$

applies and, as a result, the last term in Eq. (3) can be neglected in the first approximation. The shape factor for boundary layers with constant total temperature can be approximated as

$$H=(\overline{H}+1)\left\{1+\frac{\gamma-1}{2}M^2\right\}-1 \tag{5}$$

where $\overline{H}$ is the transformed shape factor.[4] Because $\overline{H}$ approaches one as the Reynolds number becomes large, Eq. (5) can be written as

$$H=1+(\gamma-1)M^2 \tag{6}$$

for the present problem. From Eq. (6) and the small-perturbation form of the energy equation, it follows that

$$\frac{\partial H}{\partial x}=\frac{(H-1)(H+1)}{U}\frac{\partial u}{\partial x} \tag{7}$$

Presented as Paper 81-1297 at the AIAA 14th Fluid and Plasma Dynamics Conference, Palo Alto, Calif., June 23-25, 1981; submitted July 16, 1981; revision received Jan. 13, 1982.

*Research Engineer, NTF Aerodynamics Branch. Member AIAA.

With Eqs. (3) and (7), and the inequality equation (4) applied to Eq. (1), Eq. (2) can be rewritten as

$$\bar{\beta}^2_\infty \frac{\partial u}{\partial x} + \frac{\partial v}{\partial y} = (\gamma+1)M^2_\infty \frac{u}{U}\frac{\partial u}{\partial x} \tag{8}$$

where

$$\bar{\beta} = \sqrt{1 - M^2_\infty + \frac{2\delta^*}{b}\left(2 + \frac{1}{H} - M^2_\infty\right)} \tag{9}$$

Use of constant values of δ^* and H allows direct application of von Kármán's transonic similarity rule[5] to form the sidewall similarity rule which establishes similar flowfields in the same two-dimensional tunnel with different sidewall boundary-layer thicknesses. This sidewall similarity rule provides an equivalent Mach number for an ideal two-dimensional tunnel without a sidewall boundary layer ($\delta^* = 0$) and an adjustment for the pressure coefficients from measured values to values in this ideal tunnel. This equivalent Mach number $\bar{\bar{M}}_\infty$ and the adjusted pressure coefficient $\bar{\bar{C}}_p$ can be expressed as

$$\frac{\bar{\bar{M}}_\infty}{(1-\bar{\bar{M}}^2_\infty)^{3/4}} = \frac{M_\infty}{\bar{\beta}^{3/2}} \tag{10}$$

and

$$\bar{\bar{C}}_p = (\bar{\beta}/\sqrt{1-\bar{\bar{M}}^2_\infty})C_p \tag{11}$$

where M_∞ and C_p are the measured values of Mach number and pressure coefficient in the actual tunnel. Expressions for the adjusted force coefficients can be obtained by integration of the surface pressure coefficient given by Eq. (11) as

$$\text{adjusted section normal force coefficient} = \bar{c}_n = (\bar{\beta}/\sqrt{1-\bar{\bar{M}}^2_\infty})c_n \tag{12}$$

and

$$\text{adjusted section drag coefficient} = \bar{c}_d = (\bar{\beta}/\sqrt{1-\bar{\bar{M}}^2_\infty})c_d \tag{13}$$

where c_n and c_d are the measured section normal force and drag coefficients.

An approximate expression for the increment $M_\infty - \bar{\bar{M}}_\infty$ can be formulated from the first-order Taylor series expansions of both sides of Eq. (10) as

$$M_\infty - \bar{\bar{M}}_\infty \simeq \frac{3M_\infty}{2+M^2_\infty}\left(2 + \frac{1}{H} - M^2_\infty\right)\frac{\delta^*}{b} \tag{14}$$

For M_∞ ranging between 0.7 and 0.9 and H ranging between 1.4 and 1.6, this increment is approximately

$$M_\infty - \bar{\bar{M}}_\infty \simeq 2\delta^*/b \tag{15}$$

This is the fraction of the tunnel occupied by the two sidewall displacement thicknesses.

Experimental Apparatus

To study the effect of the sidewall boundary-layer displacement thickness in a two-dimensional tunnel, the sidewall boundary layer in the Langley 6×19 in. Transonic Tunnel[6] has been successively thickened for tests on airfoil models at subsonic and transonic flow conditions. This tunnel is relatively narrow, which helps satisfy the approximation on spanwise velocity w given by Eq. (1).

The sidewall boundary layers have been artificially thickened using thin plates, each having three rows of pins protruding from the surface.[7] These plates are mounted on the sidewalls of the tunnel contraction region at 121.9 cm upstream of the model station, as shown in Fig. 1. Three pairs of plates are used in the experiment. One pair of plates has no pins, the second pair has pins 2.54 cm high, and the third pair has pins 3.8 cm high.

The boundary layers generated by these thickening devices have been surveyed at several streamwise stations along the test section centerline with total head fixed rake tube probes. These probes have tubes from the surface of the wall to about 5.10 cm away from the wall surface. The static pressure at each probe location is determined from a calibration obtained during the tunnel-empty Mach number calibration. In addition, a static temperature distribution in the boundary layer, given by[8]

$$T/T_e = 1 + 0.1793M^2_e[1 - (u/u_e)^2] \tag{16}$$

where T and T_e are the static temperatures at velocities u and u_e is assumed, so that the velocity distribution in the boundary layer can be determined using the local Mach number and static temperature at each tube location. The velocity distributions are then integrated to determine δ^* and θ, the displacement thickness and momentum thickness. For the three sidewall and boundary-layer thickening configurations tested, the displacement thickness ranged 0.20-0.78 cm and the shape factor H ranged 1.39-1.59. The transformed shape factor $\bar{H}$, which is assumed to be one in the analysis, ranged 1.18-1.26.

The skin friction coefficient c_f is obtained by applying the Preston tube calibration suggested by Allen[9] to the surface tube of the rake probe. The values of c_f are twice the wall shear stress expression in Eq. (4), ranging 0.0019-0.0024. This resulted in wall shear stress $\tau_w/\rho U^2$ ranging 0.0010-0.0012, while the values of δ^*/c [inequality Eq. (4)] are 0.014-0.052.

Description of Results

Results of boundary-layer surveys in the artificially thickened boundary layers and the unthickened boundary layer are presented in Figs. 2-4 for subsonic and transonic Mach numbers. The velocity profiles are shown in Fig. 2, and the artifically thickened boundary layers are correlated with the law of the wake[10] in Fig. 3. These results indicate that the artificially thickened boundary layers are sufficiently developed and have adequate boundary-layer similarity for the experiment. The variations of δ^* near the model station (tunnel empty) with the three different boundary-layer thickening arrangements are presented in Fig. 4. For all three boundary-layer thicknesses, the variation of δ^* with x/c is small. Therefore, the pressure gradients generated by the model should be the dominating cause of variations in the effective tunnel width, $b-2\delta^*$, that modify the continuity equation in the manner indicated by the analysis.

The effectiveness of the sidewall similarity rule has been evaluated by comparing measured airfoil test data obtained at different sidewall boundary-layer displacement thicknesses.

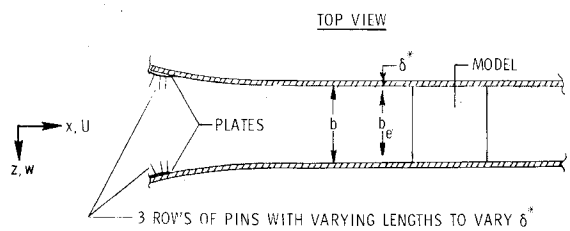

Fig. 1 Experimental apparatus used in the Langley 6×19 in. Transonic Tunnel to investigate the effects of the sidewall boundary-layer displacement thickness on two-dimensional testing.

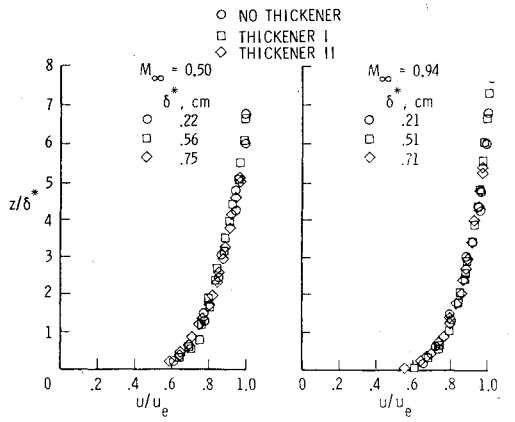

Fig. 2 Nondimensional velocity distributions in artifically thickened sidewall boundary layers.

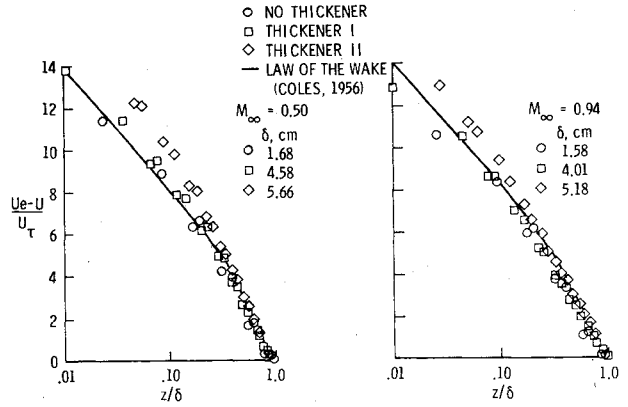

Fig. 3 Nondimensional velocity distributions for law-of-the-wake correlation of artificially thickened sidewall boundary layers.

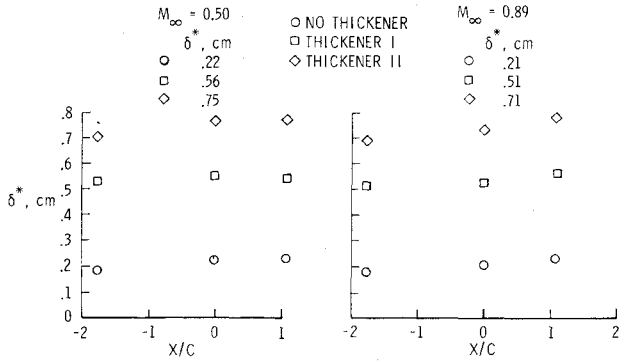

Fig. 4 Variation of the measured boundary-layer displacement thickness near the model station.

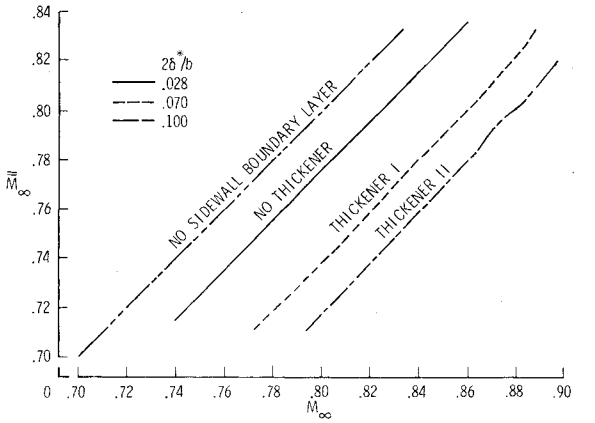

Fig. 5 Variation of equivalent Mach number with freestream Mach number for three sidewall boundary-layer displacement thicknesses.

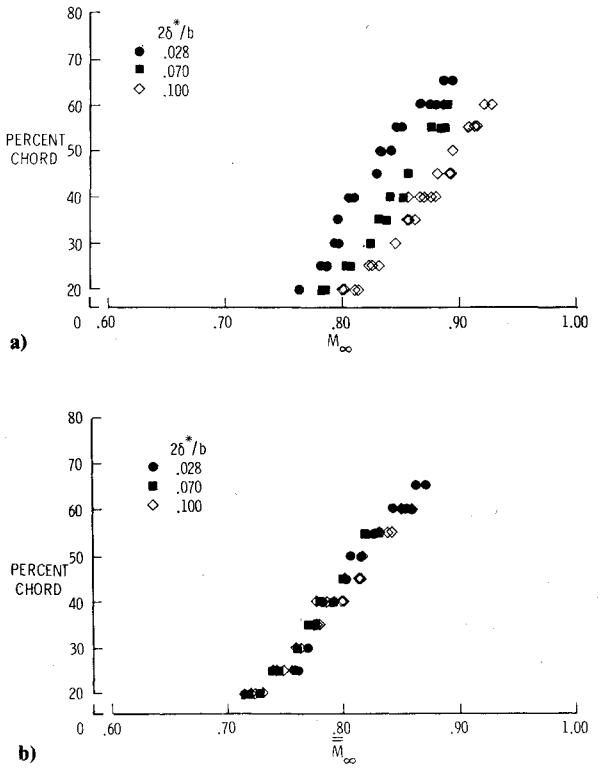

Fig. 6 Variation of shock wave location with freestream Mach number for the NACA 0012 airfoil tested with three sidewall boundary-layer displacement thicknesses: a) shock wave location vs freestream Mach number; b) shock wave location vs equivalent freestream Mach number.

First, the equivalent Mach number $\bar{\bar{M}}_\infty$ was determined for the three boundary-layer thicknesses with Eqs. (9) and (10). The values of δ^* and H used in Eq. (9) were measured at the model station. Figure 5 shows the variation of $\bar{\bar{M}}_\infty$ with M_∞ for the three boundary-layer thicknesses and shows an increment between the equivalent Mach number and the measured freestream Mach number of approximately $2\delta^*/b$ as indicated in Eq. (15).

Next, the variations of shock wave location with both M_∞ and $\bar{\bar{M}}_\infty$ were compared for the NACA 0012 airfoil at zero angle of attack with the three sidewall boundary layers. This comparison is presented in Fig. 6. A significantly improved correlation is obtained when $\bar{\bar{M}}_\infty$ rather than M_∞ is used.

Another transonic characteristic of the NACA 0012 airfoil which was used to evaluate the application of the similarity rule was the variation of the section drag coefficient at zero angle of attack with freestream Mach number. Here, the similarity rule requires the application of Eq. (13) to alter the measured drag coefficient to the adjusted drag coefficient $\tilde{c}_d$. This adjustment actually applies only to the component of pressure drag in the drag coefficient, and does not account for the skin friction component. Figure 7 shows the comparison between the measured section drag coefficient c_d plotted against M_∞ and the adjusted section drag coefficient $\tilde{c}_d$ plotted against $\bar{\bar{M}}_\infty$ for the three sidewall boundary layers. In Fig. 7, the similarity rule provides a substantially improved drag correlation in the region of drag rise, but loses quality below the drag rise. This is probably because most of the drag comes from the skin friction when below the drag rise, whereas the adjusted drag coefficient addresses only the pressure drag. The correlation improves as the pressure drag becomes a larger fraction of the total drag, as seen in the drag rise region. Figure 7 also indicates more scatter in the drag

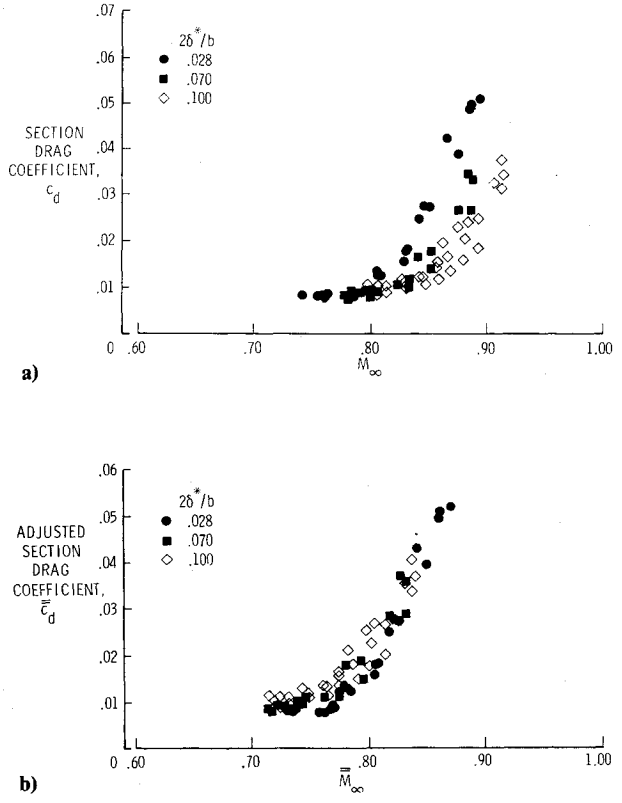

Fig. 7 Variation of section drag coefficient with freestream Mach number for the NACA 0012 airfoil tested with three sidewall boundary-layer displacement thicknesses: a) section drag coefficient vs freestream Mach number; b) adjusted section drag coefficient vs equivalent freestream Mach number.

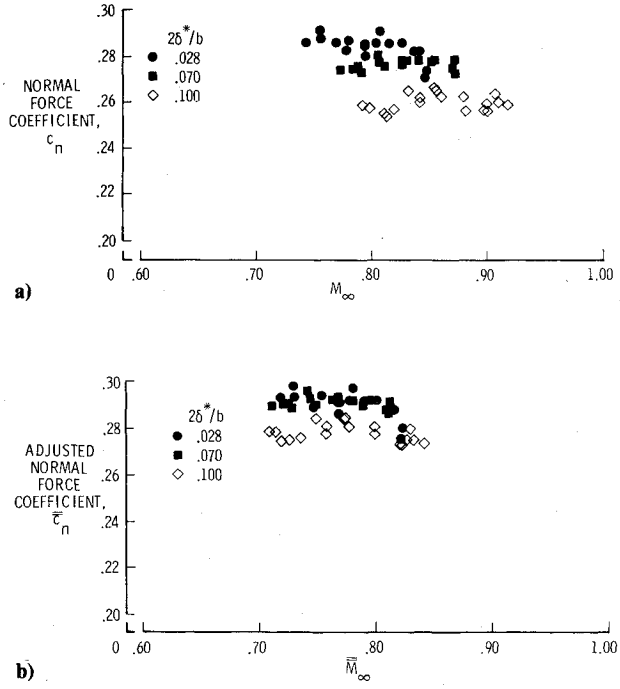

Fig. 8 Variation of section normal-force coefficient with freestream Mach number for a supercritical airfoil tested with three sidewall boundary-layer displacement thicknesses: a) section normal-force coefficient vs freestream Mach number; b) adjusted section normal-force coefficient vs equivalent freestream Mach number.

data measured with the thickest sidewall boundary layer. This boundary layer was approximately 5.2 cm thick at the model station (tunnel empty) so that the two sidewall boundary layers occupied approximately two-thirds of the tunnel width. This large amount of sidewall boundary layer probably adversely influences the drag measurements made with the wake probe.

The final characteristic investigated was the variation of the section normal-force coefficient at a fixed angle of attack with freestream Mach number. This investigation was performed with a supercritical airfoil rather than the NACA 0012 airfoil because the shock wave on a supercritical airfoil is generally much weaker than that on the NACA 0012 airfoil at lifting conditions. The use of this airfoil reduced the three-dimensional interaction between the model shock wave and the sidewall boundary layer.

For the section normal-force coefficient, the similarity rule requires Eq. (12) to be used to provide an adjusted section normal-force coefficient $\bar{c}_n$. Figure 8 shows the comparison between c_n plotted against M_∞ and $\bar{c}_n$ plotted against $\bar{M}_\infty$.

Figures 6-8 show that an improved correlation is obtained using the similarity rule, particularly for the two thinnest sidewall boundary layers. The correlation quality diminishes for the third sidewall boundary layer, probably because of its large thickness compared to the tunnel width. Therefore, the data for the thickest sidewall boundary layer are presented with open symbols, while the data for the two thinner sidewall boundary layers, where the similarity rule is more applicable, are presented with solid symbols.

Conclusion

The effects of attached sidewall boundary layers in two-dimensional tunnels have been correlated with a transonic similarity rule. It has been shown experimentally that the application of this similarity rule to the data obtained in the Langley 6×19 in. Transonic Tunnel gives an effective freestream Mach number correction. The similarity rule correction applies provided the sidewall boundary layer is small enough to avoid excessive three-dimensional interactions with the model. The similarity rule correction can be used as long as the sidewall boundary layers have no separation (due to shock-wave/boundary-layer interaction or significant trailing-edge separation).

References

[1] Preston, J. H., "The Interference on a Wing Spanning a Closed Tunnel, Arising from the Boundary Layers on the Side Walls, with Special Reference to the Design of Two-Dimensional Tunnels," NPL, Teddington, England, R&M 1924, March 1944.

[2] Winter, K. G. and Smith, J.H.B., "A Comment on the Origin of Endwall Interference in Wind-Tunnel Tests of Aerofoils," Royal Aeronautical Establishment, Tech. Memo Aero 1816, Aug. 1979.

[3] Barnwell, R. W., "Similarity Rule for Sidewall Boundary-Layer Effect in Two-Dimensional Wind Tunnels," *AIAA Journal*, Vol. 18, Sept. 1980, pp. 1149-1151.

[4] Green, J. E., "Interaction Between Shock Waves and Turbulent Boundary Layers," *Progress in Aeronautical Sciences*, Vol. XI, Pergamon Press, New York, 1970.

[5] Liepmann, H. W. and Rosko, A., *Elements of Gas Dynamics*, John Wiley & Sons, New York, 1957, pp. 256-258.

[6] Ladson, C. L., "Description and Calibration of the Langley 6- by 19-Inch Transonic Tunnel," NASA TN D-7182, 1973.

[7] Johnson, D. F. and Mitchell, G. A., "Experimental Investigation of Two Methods for Generating an Artificially Thickened Boundary Layer," NASA TM X-2238, 1971.

[8] White, F. M., *Viscous Fluid Flow*, McGraw Hill Book Co., New York, 1974, p. 627.

[9] Allen, J. M., "Evaluation of Compressible-Flow Preston Tube Calibrations," NASA TN D-7190.

[10] Coles, D., "The Law of the Wake in the Turbulent Boundary Layers," *Journal of Fluid Mechanics*, Vol. 1, 1956, pp. 191-226.